ISSN (Print) 1226-1750
ISSN (Online) 2233-6656
Journal of Magnetics 24(1), 128-134 (2019) https://doi.org/10.4283/JMAG.2019.24.1.128

Equivalent Circuit Based Design of an Integrated 2DoF Machine for Submerged Drilling Systems

Lujia Xie[1], Haichao Feng[3]*, Jikai Si[2,3], Yihua Hu[1], and Kai Ni[1]

[1]*University of Liverpool, Liverpool L69 3BX, United Kingdom*
[2]*Zhengzhou University, No.100 Science Avenue, Zhengzhou, China*
[3]*Henan Polytechnic University, No.2001 Century Avenue, Jiaozuo, China*

(Received 2 July 2018, Received in final form 26 February 2019, Accepted 28 February 2019)

Drilling is traditionally performed by multi-motor systems manually. However, the complex intermediate transmission mechanisms in the traditional design have large size and relatively low robustness. In this paper, a split-stator 2-degree-of freedom (2DoF) machine is applied. By conducting linear, rotary, and helical motion by only one machine, it provides a more compact, more integrated, more reliable, and stronger-adaptability electrically drilling machine for submerged drilling systems. On account of the adoption of the split-stator structure, the electromagnetic design of such 2DoF machine is a significant challenge. In this paper, a design method for the 2DoF machine with special split structure is proposed based on the electric decoupled equivalent circuit (EDEC). Then a 1.5 kW 2DoF drilling machine is designed, and the electromagnetic performances are verified by the 3D finite element analysis (FEA). The results show the good characteristics and feasibility of applying the 2DoF machine in drilling systems.

Keywords : 2DoF machine, submerged drilling system, machine design, finite element method

1. Introduction

Using integrated systems instead of complicated segregated systems has been on trend for the development of various industrial applications. For example, submerged applications of drilling systems are always limited by internal space yet reducing equipment volumes and mass can provide capacity for additional cargo and voyage [1]. Therefore, it is necessary to simplify the submerged drilling system, where the rotary motion, linear motion and helical motion are needed under different situations and finally contribute to the submerged industry. Traditionally, such motions are realized by one rotary motor stacked on top of another, which are mounted with rotary-to-linear transmissions converting the rotational torque to axial force [2]. As an alternative, at least one rotary motor producing rotational torque and one linear motor directly making the linear force are linked in series [3]. However, they have the defects of complicated mechanisms, enormous space requirements, frequent mechanical adjustments, high maintenance costs, and low reliability [4]. Considering energy saving and limited space of submerged environments, developing a machine to produce rotary, linear or helical movements in one compact structure is highly demanded.

Thanks to the development and innovation of new technologies, a new type of electrical machine, namely the 2-degree-of-freedom (2DoF) rotary-linear (RL) motor, which can realize rotary motion, linear motion or 3-dimentional helical motion by employing only one motor [5-7]. Compared with the traditional RL motion system, the 2DoF RL machine is much more integrated and room-saving due to the absence of intermediate mechanical devices. It has high material utilization, improved response, and low energy waste, which has a tremendous potential in submerged drilling system.

Considering the harsh working condition and demand of full load operation of the drilling system, induction-type motor is more suitable than permanent magnet motor [8]. In this paper, an integrated 2DoF drilling machine with split stator and solid mover is conceived. Although some research of 2DoF machines have been carried out

*Corresponding author: Tel: +8613462847991
Fax: +8613462847991, e-mail: fhc@hpu.edu.cn

This paper was presented at the IcAUMS2018, Jeju, Korea, June 3-7, 2018.

[9-11], the fast and effective electromagnetic design of such 2DoF machine is still a significant challenge. Therefore, an electric decoupled equivalent circuit (EDEC) based design programme is proposed in this paper according to the special split structure of the proposed machine aiming to drive submerged drilling system. The design combines corrected equivalent circuit method and the unit magnetic impedance method. Then the structure parameters of a 1.5 kW 2DoF machine are designed and analyzed. The main performances are predicted, which are coincide well with those of finite element analysis (FEA) results.

2. Structure and Principle

2.1. Structure

Figure 1 shows the overall structure of the 2DoF drilling machine. The machine consists of an integrated stator and a mover. The stator consists of two arc-shape iron cores, namely the rotary and linear motion stators. The rotary motion stator is slotted along the axial direction whereas the linear one is slotted in the circumferential direction. They have the same electromagnetic parameters and they are assembled orthogonally to form a united stator. As for the common solid mover shared by both the two stators, a double-layer structure is applied to enhance the performance of the 2DoF drilling machine. It can be seen that the solid steel is coated with a thin copper layer and the drill bit is connected directly to the mover.

2.2. Operation principle

When the rotary motion stator is energized, a rotating magnetic field will be generated. According to the electromagnetic induction principle, the voltage and current will be induced on the mover surface to produce an electromagnetic torque. Then the drill bit will produce rotary motion. Similarly, a traveling wave magnetic field will be generated to create a force when the linear motion stator is powered, and then the drill bit realizes linear motion.

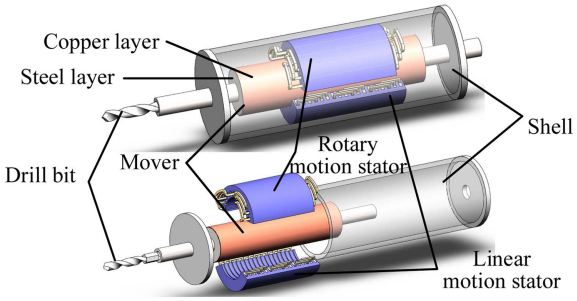

Fig. 1. (Color online) overall structure of the 2DoF drilling machine.

Therefore, the drill bit will produce single mechanical motion (single degree), when either the rotary or linear motion stator is energized, whereas the helical motion can be obtained by the both stators energized synchronously.

3. 2DoF Machine Design

As mentioned earlier, the solid mover is adopted by the 2DoF drilling machine. This kind of structure has the merits of reduced inrush starting current, simplified topology, low manufacturing cost of the mover, high reliability, robust mechanical strength, and low vibration as well as acoustic noise level [12]. Therefore, it is a potential candidate for the drilling machine applications, especially in submerged system with harsh environment.

Except of having the characteristics of the solid-mover induction motor, the 2DoF drilling machine, which adopts split-stator structure, can be equivalent to an unrolled flat linear motor, as shown in Fig. 2. In this way, the design of the 2DoF drilling machine is developed based on a combination of the solid-mover induction motor and flat linear induction motor.

In order to predict the performance such as efficiency, power factor, and output torque of the 2DoF drilling machine in a short period of time, an electric decoupled equivalent circuit (EDEC) based design programme is developed. However, on account of the split-stator structure of the 2DoF drilling machine as shown in Fig. 1,

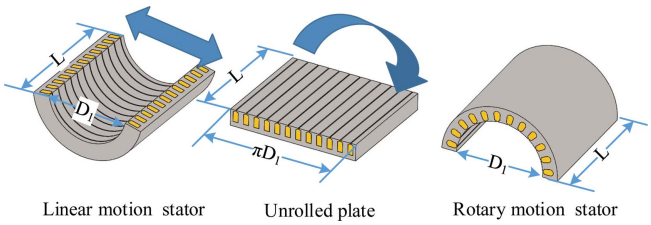

Fig. 2. (Color online) Equivalent transformation.

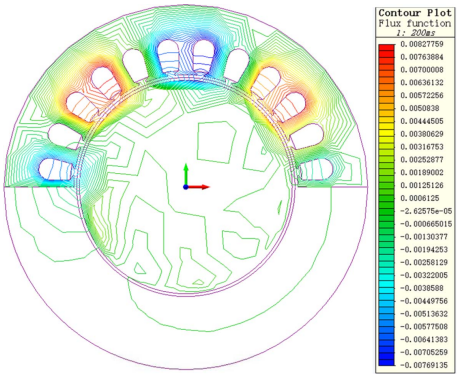

Fig. 3. (Color online) Magnetic flux distribution of the rotary motion part.

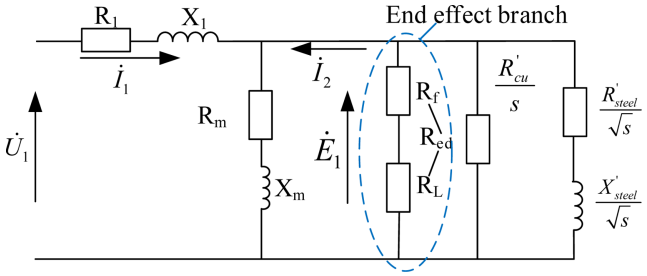

Fig. 4. (Color online) Corrected equivalent circuit of rotary motion part of the 2DoF drilling machine.

the end effect cannot be ignored. It will tend to resist a sudden increase in flux penetration and only allow a gradual build up of flux density in the airgap shown in Fig. 3 (rotary motion part). The influence can be quantified by examining the magnetizing branch of the equivalent circuit [13]. Thus, compared with that of the traditional rotary squirrel-cage motor, the equivalent circuit of the rotary motion part is corrected by adding a branch of the end effect as shown in Fig. 4. Moreover, the two branches of copper and steel layers are also added for including the characteristics of the double-layer solid-mover.

In Fig. 4, R_1, R_m, and X_1, X_m are the resistance and reactance of the primary winding and the excitation, respectively. The branch of R_{ed} is used to consider the end effect, where, R_f and R_L are the calculating resistances respecting to the loss produced by the resistant torque and the net power loss of the vertical end effect, respectively. The branches of R'_{cu}/s, $R'_{steel}/\sqrt{s}$ in series with $X'_{steel}/\sqrt{s}$ represent the copper layer and steel layer of the mover, respectively.

Based on the equivalent circuit in Fig. 4, the flow chart of the design programme can be obtained as shown in Fig. 5, where H_e is the tangential magnetic field intensity of mover surface, I_1 and E_1 are the root mean square values of the stator current and induced electromotive force. T_{st}, $\cos\varphi_{st}$, η_{st}, and P_{1st} are the output torque, power factor, synchronous efficiency, and input power respectively at the machine starting state. G is the goodness factor, $G = X_m/R'_2$. J_{1st}, $B_{\delta st}$, and A_{1st} is the current density, flux density in airgap area and electric load, respectively.

Firstly, the original design dimensions are determined including outside diameters, axis length, etc. as listed in Table 1. Then, the reasonable number of turns and diameter of the coil are calculated referring to the original current density and air-gap magnetic flux density [14]. Further, magnetomotive forces of the yoke F_j, tooth F_t, airgap F_δ and whole $\sum F$ ($\sum F = F_j + F_t + F_\delta$) areas of the machine are derived by iterative computations. Finally,

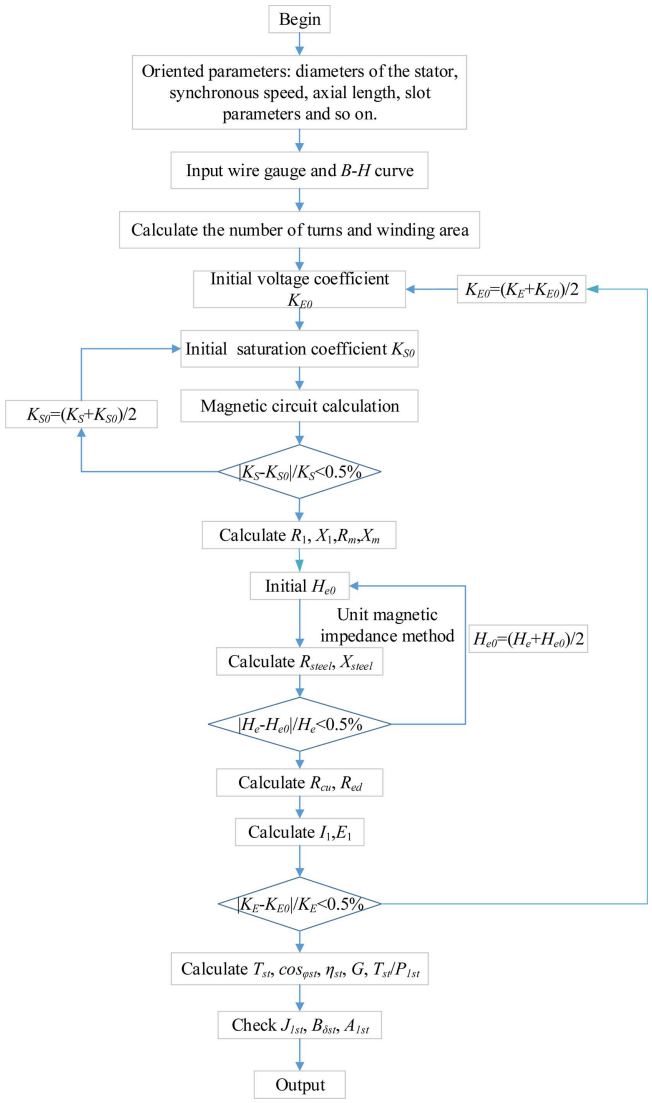

Fig. 5. (Color online) Flow chart of the design programme.

after meeting the demand of the voltage coefficient K_E and the saturation coefficient K_S ($K_S = \sum F/F_\delta$), the characteristic parameters of the machine, such as output torque and power factor, can be obtained based on the equivalent circuit in Fig. 4.

The unit magnetic impedance method [15] is applied to calculate the parameters of the steel layer R'_{steel} and X'_{steel} in equivalent circuit Fig. 4.

$$R'_{steel} = Z'_{steel}\cos 36^\circ, X'_{steel} = Z'_{steel}\sin 36^\circ \quad (1)$$

Where, Z'_{steel} is the equivalent impedance of the steel layer and 36° is the empirical value of the impedance angle.

$$Z'_{steel} = \frac{4\pi\sqrt{f}}{|Z_m|}\frac{m_1(N_1K_{dp1})^2}{p}\frac{L_{ef}}{\tau}K_r \quad (2)$$

Where, f is the frequency, m_1 is the number of phases, N_1 is the number of turns, K_{dp1} is the winding factor, L_{ef} is effective length of the motor, p is the number of pole pairs and τ is the pole distance. Z_m is the calculated unit impedance, which is derived by the curve of unit impedance vs. magnetic field intensity [15]. K_r is the transverse end effect coefficient, $K_r = 1 + 2\tau / (\pi L_{ef})$.

For the branch of the longitudinal end effect,

$$\begin{cases} R_{ed} = r_{ed} \dfrac{1}{s^2 + 3.38}, \\ R_f = r_{ed} \dfrac{s(1-s)}{(s^2+3.38)^2}, R_l = r_{ed} \dfrac{2s^2 - s + 3.38}{(s^2+3.38)^2} \end{cases} \quad (3)$$

Where, $r_{ed} = \dfrac{7.5(2p+0.3)^2 \sqrt{s} R'_{steel}}{m_1 K_{dp1}^2 p}$ and s is the slip.

For the branch of the copper layer,

$$R'_{cu} = \frac{2K_r \rho_{cu} m_1 (N_1 K_{dp1})^2 L_{ef}}{(\pi((D_{cu}/2)^2 - (D_{steel}/2)^2))/2} \quad (4)$$

Where, ρ_{cu} is the resistivity of copper, D_{cu} and D_{steel} are outer diameters of copper and steel layers, respectively.

For the rotary motion part of 2DoF machine, the synchronous power is determined as 1.5 kW and the key design parameters are listed in Table 1. Based on the EDEC design method, the circuit parameters of the rotary motion part in Fig. 4 are deduced as shown in Table 2, and then the key parameters torque T_{st}, stator current I_{1st} and power factor $\cos\varphi_{st}$ can be obtained as listed in Table 4.

Table 1. Design results of the rotary motion part.

Items	Values
Inner diameter D_{i1} (mm)	80
Outer diameter D_{i2} (mm)	130
Number of slots Z_1	12
Number of poles $2p$	4
Slots per pole per phase q	1
Number of turns N_1	95
Wire diameter D_coli1 (mm)	0.67
Pole pitch τ (mm)	31.4
Axial length L_1 (mm)	120
Air-gap thickness d_δ (mm)	1
Rated voltage U_N (V)	220
Rated frequency f (Hz)	50
Rated current I_{N1} (A)	9
Number of phases m_1	3
Number of parallel wound N_{t1}	1
Goodness G	1.9163
Current density of the windings J_1 (A/mm^2)	6.46
Magnetic flux density in air-gap B_δ (T)	0.3647
Specific electric load A_1 (A/m)	21400A
Copper thickness d_{cu} (mm)	1

Table 2. Circuit parameters of the rotary motion part.

Items	Values
Stator resistance R_1 (Ω)	4.6518
Stator reluctance X_1 (Ω)	4.5141
Excitation resistance R_m (Ω)	0
Excitation reluctance X_m (Ω)	11.5409
Resistance of copper layer R'_{cu} (Ω)	6.2763
Resistance of steel layer R'_{steel} (Ω)	127.3628
Reluctance of steel layer X'_{steel} (Ω)	92.5345
Resistance of end effect R_{edst} (Ω)	471.2065

Table 3. Main structure parameters of the linear motion part.

Items	Values
Inner diameter D_{i1} (mm)	80
Outer diameter D_{i2} (mm)	130
Number of slots Z_2	12
Number of poles $2p$	4
Slots per pole per phase q	1
Number of turns N_2	44
Wire diameter D_coli2 (mm)	0.85
Air-gap thickness d_δ (mm)	1
Rated voltage U_N (V)	220
Rated frequency f (Hz)	50
Rated current I_{N2} (A)	10
Number of phases m_2	3
Number of parallel wound N_{t2}	1
Pole pitch τ_2 (mm)	35
Axial length L_2 (mm)	140
Copper thickness d_{cu} (mm)	1

In combination of structure parameters of the rotary motion part, the linear motion part is also developed based on the design method. Table 3 listed the main parameters of the linear motion part, where the arc of the

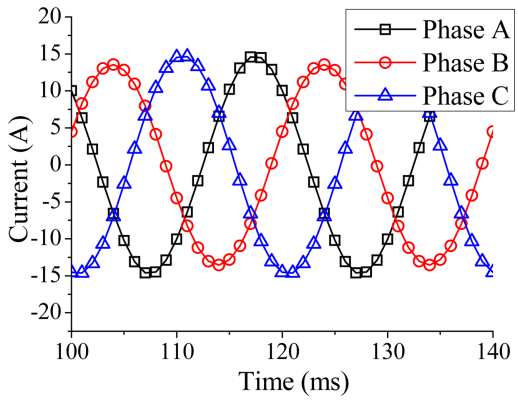

Fig. 6. (Color online) Stator currents of the rotary motion (s = 1).

Table 4. Results co.mparison of the FEM and design programme ($s = 1$).

Item	Design Programme	FEM	Error
Torque T_{st} (Nm)	17.90Nm	15.64Nm	14.45 %
Stator current I_{1st} (A)	10.88A	10.06A	8.15 %
Power factor cosφ	0.796	0.74	7.57 %
Synchronized efficiency η_s (%)	49.1	43.4	13.11 %
Input power P_{in} (W)	3259.38W	2829.47W	13.46 %
Copper loss of stator P_{Cu1} (W)	1653.2W	1442.65W	14.59 %

linear motion armature is chosen as 150° and the axial length of the linear motion armature is set as 140 mm. Such arrangement can leave room for the end windings of the rotary and linear motion parts, as well as reduce crossings between rotary and travelling-wave magnetic fields. In addition, the double-layer windings are applied in linear motion part.

To verify the EDEC design method, the electromagnetic performances of 2DoF machine are investigated by 3D-FEA. Fig. 6 shows the stator currents of the rotary motion at local mover condition. It can be seen that the three phases currents are unbalanced, which is caused by the cutting of primary iron core and discontinuity of the windings. The FEA results are compared with those of the EDEC design method as shown in Table 4.

It can be seen that the errors between FEA and EDEC are less than 15 %. Therefore, the EDEC design method can be used to the process of the preliminary design of the drilling machine. It can be found that the output torque at locked mover condition is 15.64Nm, and the current is 10.06A. Fig. 7, Fig. 8 and Fig. 9 show the torque, stator current, and power factor at different slip of the rotary motion derived by FEA and the EDEC design method.

It can be seen from Fig. 7, Fig. 8 and Fig. 9 that the torque, current and power factor increase as the slip rises, and the overall error between FEA and EDEC based

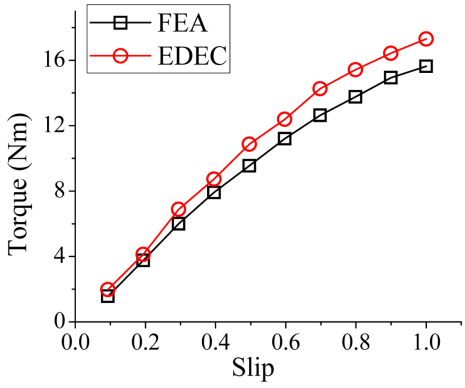

Fig. 7. (Color online) Torque vs. slip of the rotary motion.

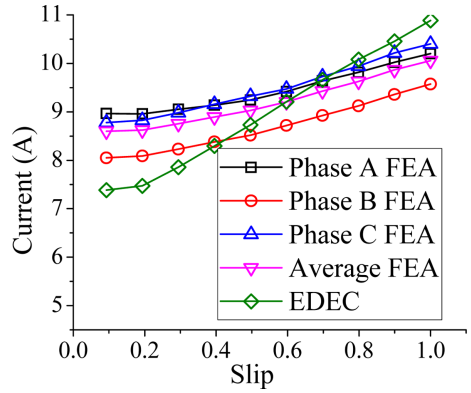

Fig. 8. (Color online) Stator current vs. slip of the rotary motion.

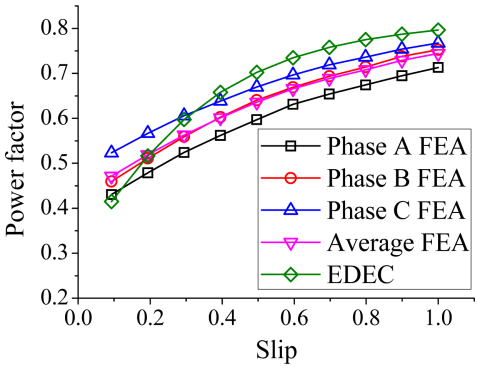

Fig. 9. (Color online) Power factor vs. slip of the rotary motion.

design programme is less than 15 % and the drilling machine can achieve rotary motion. Moreover, according to Fig. 8, as the load increases, the stator currents of the 2DoF drilling machine increases slightly, which is one particular advantage for drilling applications. In addition, compared with other classical solid-rotor machines with poor power factor [14], the power factor of the 2DoF drilling machine is higher than 0.5 when the slip is bigger than 0.2 according to Fig. 9.

Similarly, the characteristics of linear motion part is also investigated. Fig. 10 shows the magnetic field distribution of the linear motion part. Fig. 11, Fig. 12 and Fig. 13 show the output forces, stator currents, and power

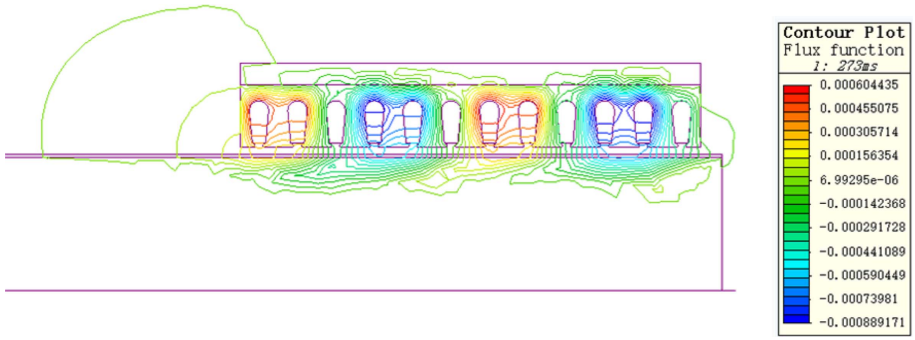

Fig. 10. (Color online) Magnetic flux distribution of the linear motion part.

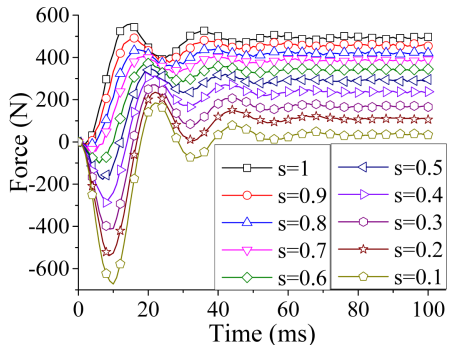

Fig. 11. (Color online) Force vs. slip of the linear motion.

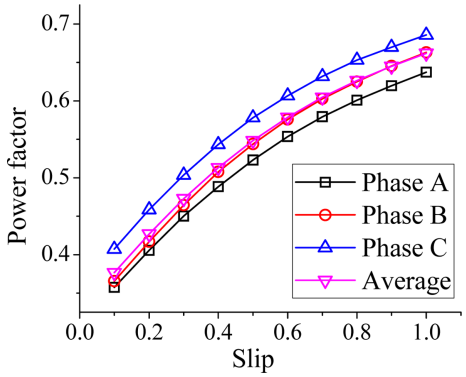

Fig. 13. (Color online) Power factor vs. slip of the linear motion.

factors at different slip of the linear motion part. Moreover, the average output force is presented in Table 5. According to the 3D-FEA results, the feasibility of the linear motion of the 2DoF machine is validated. The steady output force fluctuates within 5 % (10 % when slip is 0.1), which satisfied the design requirements. With the increase of the slip, the force, current and power factor increase and the ratio of the output force (N) and input power (kW) can reach as much as 168. Therefore, the linear motion operates well in the state of low speed and high force, which is suitable for the application in a submerged drilling tool.

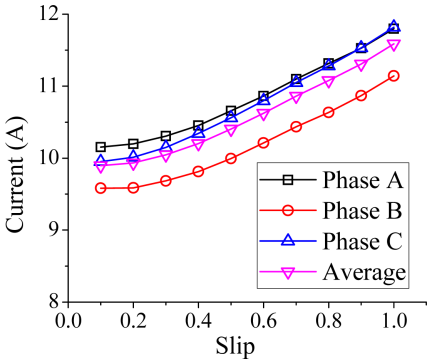

Fig. 12. (Color online) Stator current vs. slip of the linear motion.

4. Conclusion

In this paper, implementation of 2DoF machine on submerged systems is presented and a split-stator structure of the 2DoF drilling machine is developed. It can achieve rotary, linear or helical motion by only one motor. The preliminary parameters of the 2DoF machine is designed based on the EDEC method, where the end effect is considered in the design progress of both rotary and linear motion parts. The electromagnetic performances including torque, power factor and stator current under different slip are predicted, and then the results are verified by the 3D-FEA. It can be found that the designed

Table 5. Average force vs. slip of the linear motion.

Slip	0.1	0.2	0.3	0.4	0.5	0.6	0.7	0.8	0.9	1
Force (N)	36.03	110.75	168.31	237.55	292.32	340.11	386.60	420.44	457.30	492.14

2DoF machine satisfies the performance requirements, and simplifies the driving system effectively, which is suitable for the drilling application.

Acknowledgement

This work is supported by National Natural Science Foundation of China under grant no. 51777060 and no. 51277054, Henan Natural Science Foundation of China under grant 162300410117.

References

[1] Y. Wang, W. Xuhui, L. Zhang, and Z. Jian, Int. Conf. on Electrical Mach. and Syst. (ICEMS), 1 (2011).
[2] T. T. Overboom, J. W. Jansen, E. A. Lomonova, and F. J. F. Tacken, IEEE Trans. Ind. Appl. **46**, 2401 (2010).
[3] J. F. Pan, Y. Zou, and N. C. Cheung, IEEE Trans. Magn. **50**, 761 (2014).
[4] L. Hua, J. Xu, and Q. Xiaolong, Chinese Control and Decision Conf. (CCDC), 3259 (2016).
[5] E. Mendrela, Rozpr. Electrotech **2**, 383 (1976).
[6] E. Mendrela, Rozpr. Electrotech **2**, 385 (1979).
[7] R. Paul, IEE Journal on Electric Power Appl. **2**, 135 (1979).
[8] O. Dobzhanskyi, E. Amiri, and R. Gouws, 2ed Int. Young Scientists Forum on Applied Physics and Engineering (YSF), 14 (2016).
[9] J. Si, H. Feng, L. Ai, Y. Hu, and W. Cao, IEEE Trans. Energy Conv. **30**, 1200 (2015).
[10] J. Si, L. Xie, J. Han, H. Feng, W. Cao, and Y. Hu, Journal of Electrical Eng. & Tech. **12**, 1227 (2017).
[11] J. Si, L. Xie, X. Xu, Y. Zhu, and W. Cao, IET Electric Power Appl. **11**, 532 (2017).
[12] J. F. Gieras and J. Saari, IEEE Trans. Ind. Elec. **59**, 2689 (2012).
[13] J. Duncan, IEE Proceedings B-Electric Power Appl. **130**, 51 (1983).
[14] H. A. Toliyat and G. B. Kliman, Handbook of Electric Motors, 2nd ed. CRC Press (2004).
[15] X. Tang, Y. Ning, and F. Fu, Solid-rotor inducion motor and its applications. Beijing: China Machine Press (1991).